Materials Science & Engineering A 638 (2015) 20–29

Contents lists available at ScienceDirect

Materials Science & Engineering A

journal homepage: www.elsevier.com/locate/msea

The role of microstructure and texture in controlling mechanical properties of AZ31B magnesium alloy processed by I-ECAP

Michal Gzyl [a,*], Andrzej Rosochowski [b], Sonia Boczkal [c], Lech Olejnik [d]

[a] Advanced Forming Research Centre, University of Strathclyde, 85 Inchinnan Drive, Renfrew PA4 9LJ, United Kingdom
[b] Design, Manufacture and Engineering Management, University of Strathclyde, James Weir Building, 75 Montrose Street, Glasgow G1 1XJ, United Kingdom
[c] Institute of Non-Ferrous Metals in Gliwice, Light Metals Division, ul. Pilsudskiego 19, 32-050 Skawina, Poland
[d] Institute of Manufacturing Processes, Warsaw University of Technology, ul. Narbutta 85, 02-524 Warsaw, Poland

ARTICLE INFO

Article history:
Received 23 March 2015
Received in revised form
14 April 2015
Accepted 16 April 2015
Available online 27 April 2015

Keywords:
Magnesium alloys
Equal channel angular pressing (ECAP)
Severe plastic deformation (SPD)
Ultra-fine grained (UFG) material
Electron backscatter diffraction (EBSD)

ABSTRACT

Mechanical properties of AZ31B magnesium alloy were modified in this work by various processing routes of incremental equal channel angular pressing (I-ECAP) followed by heat treatment. Possible strategies for improving ductility and strength of the alloy were investigated. Processing by routes A and B_C showed that texture plays predominant role in controlling mechanical properties at room temperature. Four passes of I-ECAP by route C followed by annealing enhanced ductility up to 0.35 of true strain. It was found that tensile twinning was important in accommodating strain during tensile testing, which resulted in a very good hardening behaviour. The yield strength was improved to 300 MPa by refining grain size to 0.8 μm in I-ECAP at 150 °C. The obtained structure and properties were shown to be stable up to 150 °C. True strain at fracture was increased to 0.2 after annealing at 150 °C without lowering strength.

1. Introduction

Modern lightweight materials are dynamically entering new markets. Especially the aerospace and automotive sectors are taking advantage of fuel savings due to weight reduction [1,2]. Magnesium alloys are of special interest because of their low density (~1.7 g/cm^3) and a high specific strength, defined as a ratio of strength to density. However, the yield stress of magnesium alloys is still lower than commonly used aluminium alloys, which indicates that more research is needed in this field. Moreover, magnesium alloys suffer from limited formability, especially at room temperature, and low corrosion resistance. However, the latter can be also an advantage as they have been shown to be fully dissolvable within human body, which makes them promising materials for biodegradable implants with a higher strength than currently used polymers [3].

One of the possible approaches to improve strength of metals and alloys is to reduce their grain size by severe plastic deformation (SPD). Equal channel angular pressing (ECAP) [4,5] is among the most developed SPD processes used worldwide. The concept of ECAP is to press a billet through an angled channel without changing billet's dimensions. Strain introduced by simple shear at the channel's intersection usually results in significant grain refinement. Therefore, it can be used to produce materials with a submicron grain size, commonly known as ultrafine-grained (UFG) metals. However, conventional ECAP is not able to produce continuous billets as friction in the channel rises dramatically with the length of a billet. Rosochowski and Olejnik proposed a solution to this problem by separating stages of feeding and plastic deformation [6]. In their cyclic process, called incremental ECAP (I-ECAP), the billet (bar [7], plate [8] or sheet [9]) is delivered in consecutive steps to the deformation zone and a punch, moving in a reciprocating manner, deforms a small volume of material by simple shear in each cycle.

Conventional ECAP was shown to be effective in improving room temperature ductility [10], strength [11] and corrosion resistance [12,13] of magnesium alloys. However, the effect of grain refinement on mechanical properties is not clear as some researchers reported decrease in strength [14,15] while it was possible to improve yield stress in some other cases [16]. It was also emphasized that texture produced during ECAP cannot be neglected due to hexagonal close-packed (hcp) crystallographic structure of the studied alloys [15,17]. Grain size produced by ECAP can be controlled by changing processing temperature while different textures are generated by different processing routes, known as A, B_C and C. Route A indicates processing without rotation of a billet between subsequent passes of ECAP, route B_C means that the billet is rotated by 90° always in the same sense before putting back into the inlet channel and, finally, the billet is rotated by 180 °C in the case of route C. The mean grain sizes reported in different studies for various ECAP temperatures was

* Corresponding author.
E-mail address: michal.gzyl@strath.ac.uk (M. Gzyl).

http://dx.doi.org/10.1016/j.msea.2015.04.055

0.37 μm at 115 °C [11], 1 μm at 150 °C [18], 2 μm at 200 °C [11,19], and 6 μm at 250 °C [15]. Recent results obtained for I-ECAP of AZ31B confirmed that grain refinement at 250 °C is similar to that obtained by ECAP (~5–6 μm) and texture generated by using different processing routes influences strength and tension–compression asymmetry of the yield stress [20]. Despite a lot of research conducted in this field, some questions still remain unanswered. The following issues are addressed in this work:

1. What influences mechanical properties more, grain size or texture?
2. How can room temperature ductility be improved by a heat treatment after I-ECAP and what are deformation mechanisms supporting enhancement of elongation?
3. How can strength of magnesium alloy be improved by I-ECAP without lowering its ductility?

2. Material

The most common wrought magnesium alloy AZ31B (Mg–3%Al–1%Zn–0.5%Mn) was used in the current study. Billets for I-ECAP experiments were machined from a hot-extruded rod and a hot-rolled plate along extrusion and rolling directions, respectively. The bar was supplied in as-fabricated conditions (AZ31B-F) while the plate was delivered in annealed state (AZ31B-O) by Magnesium Elektron (Manchester, UK), in accordance with ASTM-B107 and ASTM-B90, respectively. EBSD analysis revealed that both materials exhibited significantly different grain sizes, bimodal structure 10 μm/50 μm for the rod and 8 μm for the plate. It is apparent from Fig. 1 that microstructure of the rod is much more heterogeneous than microstructure of the plate. The extruded rod is dominated by coarse grains as large as 70 μm surrounded by colonies of small grains with an average size of 10 μm (Fig. 1a). Microstructure of the plate is homogenous with only little fraction of coarse grains ~30 μm (Fig. 1b). Textures shown in Fig. 1(c and d) are usual fibre textures observed after extrusion and rolling of magnesium alloys. It is apparent that *c*-axes of hexagonal cells are aligned perpendicularly to the directions of extrusion as well as rolling.

3. Experimental procedure

3.1. Details of I-ECAP

Double billet variant of I-ECAP [21] with a die angle of 90° was carried out in this work on a 1 MN hydraulic servo press. A pair of billets, with cross-sectional dimensions $10 \times 10\ mm^2$ each, was fed using a motor driven screw jack whose action was synchronized with the reciprocating movement of the punch. Process parameters were the same as in the previous work on I-ECAP of AZ31B [20]: feeding stroke – 0.2 mm, punch movement frequency – 0.5 Hz, peak-to-peak amplitude of the punch movement – 2 mm. The heating of billets was realised by holding them for 15 min prior to processing in the preheated die. The die temperature during processing was kept constant within ±2 °C, based on the readings obtained from a thermocouple located 15 mm from the deformation zone.

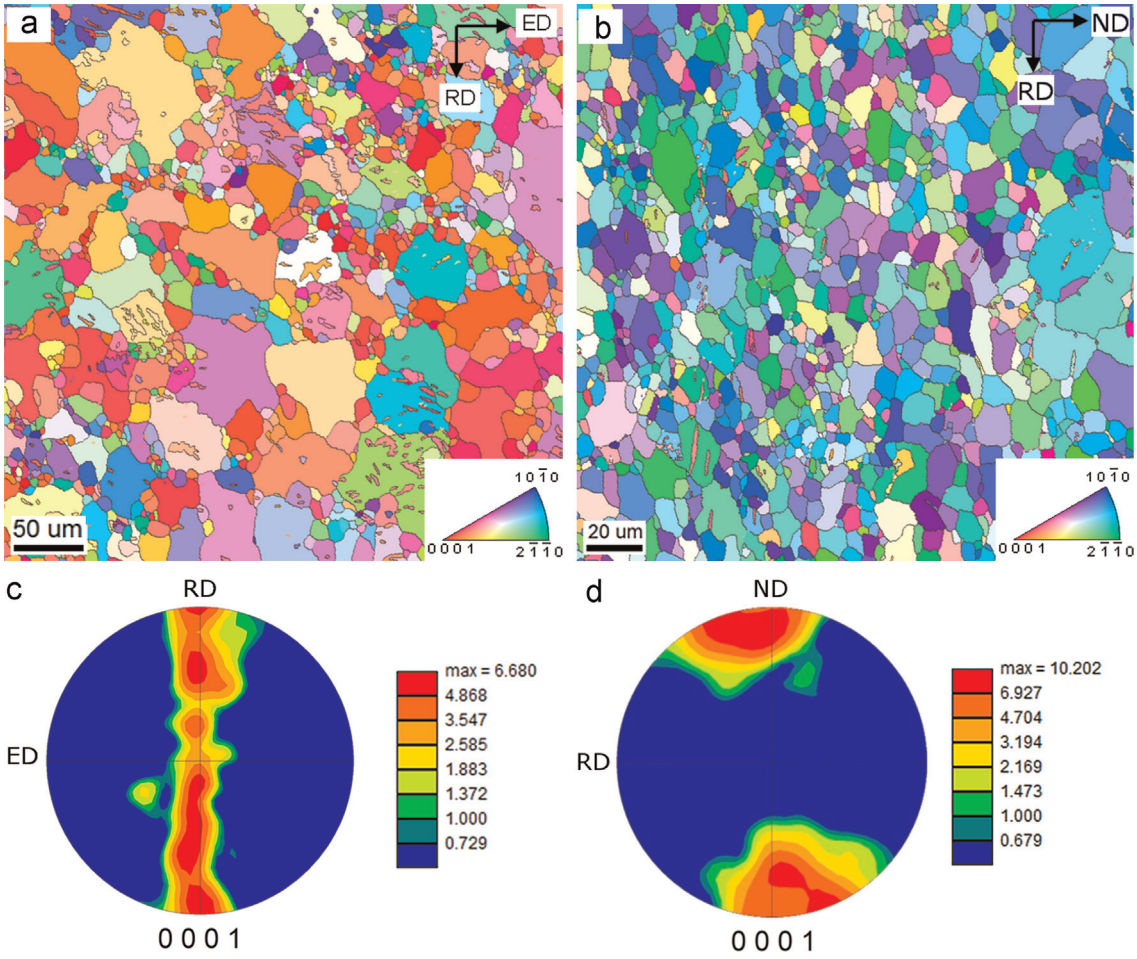

Fig. 1. Microstructures and textures of as-supplied extruded rod (a,c) and rolled plate (b,d). Symbol explanation: ED – extrusion direction; ND – normal direction of the plate; RD in image (c) – radial direction of the rod; RD in image (d) – rolling direction of the plate.

Table 1
Experimental plan of work conducted in this study.

	Initial state	Initial grain size, μm	No. passes	Route	Temperature[a],°C	Comments
Part 1	Extruded	10/50 (bimodal)	4, 6	A, B_C	250, 200	Initial four passes at 250 °C
Part 2	Extruded	10/50(bimodal)	4	C	250	Additional annealing at 300 °C
Part 3	Rolled	8	4	A	150	Initial two passes at 200 and 175 °C, additional annealing at 150, 200, 250, and 300 °C

[a] Temperature in the final pass.

3.2. Experimental plan

The experimental campaign was divided into three parts in order to address the research questions stated in Section 1; details of experiments are shown in Table 1. In the first part, billets were subjected to I-ECAP at 250 °C and 200 °C using two different routes, A and B_C. It was assumed that different temperatures will result in different grain refinement while the used routes will produce different textures. Four pairs of billets machined from the extruded rod were firstly subjected to four passes at 250 °C; then, two of them were processed by additional two passes at 200 °C. Conducting first pass at 200 °C was not possible due to the occurrence of fracture.

The second part of the experimental plan was focused on improving room temperature ductility. Our previous research has confirmed that route C generates texture which results in improved elongation compared to the initial extruded rod [20]. Additionally, route C was shown to produce more symmetrical billets than route B_C, which exhibited very similar mechanical properties. Therefore, the billets were subjected to four passes of I-ECAP by route C at 250 °C. Thereafter, they were annealed for 6 h at 300 °C. Microstructures after I-ECAP, subsequent heat treatment and tensile deformation were characterized using optical microscope and EBSD.

Strength improvement of AZ31B was attempted in the third part of the experimental campaign. In order to achieve this goal, gradual temperature reduction in consecutive I-ECAP passes was used. Following our previous study [22], which revealed the effect of initial grain size on formability during I-ECAP, a fine-grained plate of AZ31B was selected as the initial material. Route A was used in this part as it was shown to be less prone to fracture than routes B_C and C. The I-ECAP procedure was as follows: 1 pass at 200 °C, 1 pass at 175 °C, 2 passes at 150 °C. Additionally, the I-ECAPed billets were annealed for 1 h at 150, 200, 250, and 300 °C to investigate the effect of annealing temperature on mechanical properties and grain size. In particular, ductility enhancement without strength loss was sought. Annealing time was shortened to 1 h as first results showed that there was no difference in terms of grain size and mechanical properties between 1 and 6 h.

3.3. Microstructural characterization and mechanical testing

Microstructural characterization was performed on Olympus GX51 optical microscope and HRSEM Inspect F50. The as-received specimens were characterized along extrusion and rolling directions. Preparation for optical microscopy included grinding using SiC paper P1200, mechanical polishing using polycrystalline suspensions with particle sizes: 9, 3, and 1 μm, and final polishing with colloidal silica. Specimens were etched using acetic picral. Samples for EBSD were prepared by ion milling on Leica RES 100. Scans were performed with steps 0.3 μm and 0.7 μm and area sizes $200 \times 200\ \mu m^2$ and $400 \times 400\ \mu m^2$, respectively. The larger area was examined only in the case of coarse-grained rod to obtain more reliable data for statistical analysis. The EBSD analysis was performed on the ED–ND plane, as indicated in Fig. 2. Tensile flow stress curves were obtained on Instron 5969 machine with the maximum load capacity of 50 kN. Tests were carried out at room temperature, with the initial strain rate $1 \times 10^{-3}\ s^{-1}$ using 2 mm thick flat specimens with strain gauge dimensions 3 mm × 12 mm.

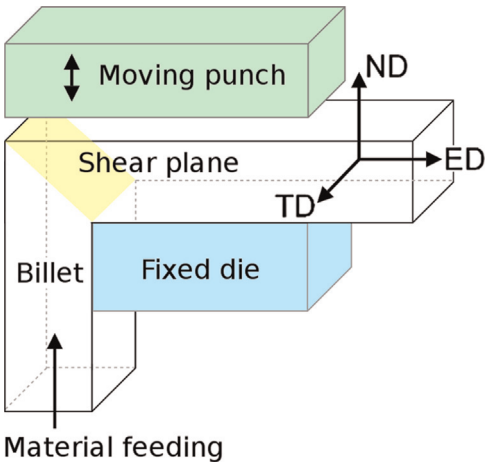

Fig. 2. Schematic illustration of I-ECAP with the main direction indicated: ED – extrusion direction, ND – normal direction, TD – transverse direction.

4. Results

4.1. Microstructures and textures

Referring to the first part of the experimental programme, the average grain size of initially coarse-grained sample was refined to 4 μm by four I-ECAP passes at 250 °C by route A (Fig. 3a). The structure was relatively homogenous as standard deviation of the measurement was 1.4 μm. Temperature reduction to 200 °C in subsequent two passes led to further grain refinement to 2.5 μm (standard deviation 1 μm), as shown in Fig. 3b. As expected, smaller grain size was obtained at lower temperature. It is apparent from Fig. 3c that texture after four passes at 250 °C is very similar to that obtained after rolling of magnesium alloys (Fig. 1d) with *c*-axes tilted at $90 \pm 15°$ to ED in the I-ECAPed billet. Processing at 250 °C/200 °C have not changed the texture significantly, as shown in Fig. 3d. Two overlapping peaks, indicating hcp cells tilted at 75° and 62° with respect to ED, can be distinguished on (0001) pole figure with maximum intensity of 11.4.

Processing by route B_C led to slightly less effective grain refinement at 250 °C than by route A as the grain size obtained from EBSD was 5 μm (Fig. 4a). Moreover, structure was also more heterogeneous since standard deviation was 3.1 μm. Texture measurement of the sample revealed that hcp cells were tilted at 52° with respect to ED (Fig. 4c). Temperature reduction refined grain size to 2.6 μm (standard deviation 1.2 μm) but texture has not been changed significantly, hcp cells are tilted at 57° and maximum intensity increased from 16.1 to 19.5 (Fig. 4b and d).

Results obtained in the second part led to the conclusion that microstructure after four passes of I-ECAP at 250 °C via route C was similar to that obtained using route B_C as the mean grain size was 4.5 μm. Standard deviation of 2.3 μm was also relatively high

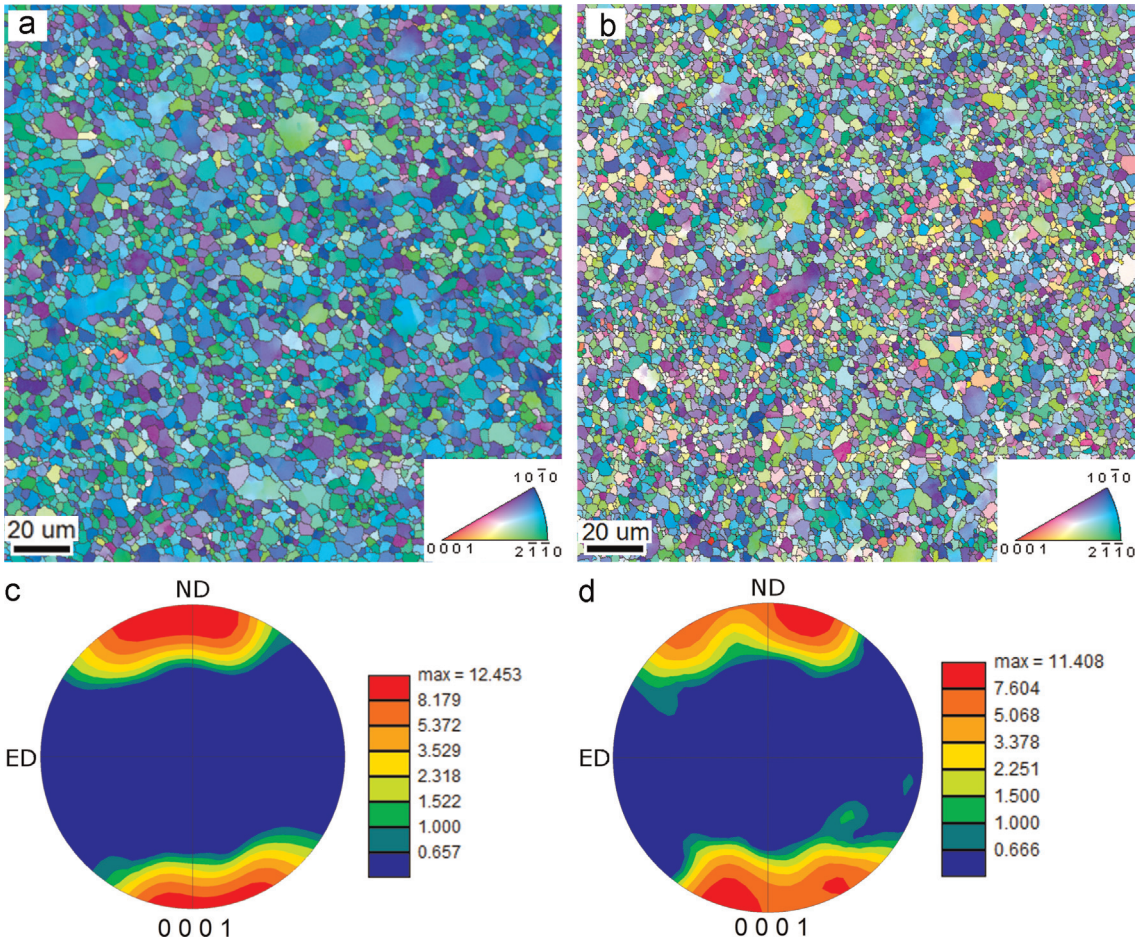

Fig. 3. EBSD maps and corresponding micro-textures of extruded samples after I-ECAP at 250 °C (a) and (c) and at 250 °C/200 °C (b) and (d) using route A.

with a necklace-like structure displayed in Fig. 5a. Heat treatment for 6 h at 300 °C did not change the grain size significantly as it was increased to 6 μm; however, it is apparent from Fig. 6c that structure became more homogenous as colonies of small grains were no longer present. Microstructure characterization of tensile samples pulled to true strain of 0.15 revealed many shear bands parallel to shear plane of I-ECAP (Fig. 5b). It is not a new finding as we have already reported similar bands in I-ECAPed samples processed by routes A, B_C and C [20]; it has been also shown in the same article that fracture in tensile samples took place along those shear planes. Deformation mechanism in the annealed sample was different from that in the as-processed sample since severely twinned structure was observed after pulling to true strain 0.15 (Fig. 5d).

In the first part of the experimental campaign, the average grain size obtained after I-ECAP at 250 °C via route A was ~4 μm and further refinement to 2.5 μm was achieved by lowering temperature to 200 °C. In the third part of the programme, using a rolled plate as the initial material, gradual reduction of temperature from 200 °C in the first pass to 175 °C in the second pass and to 150 °C in the final two passes produced an alloy with a submicron structure of 0.8 μm (Fig. 6a). Texture produced using this procedure was similar to the sample processed for six passes via route A at 250 °C/200 °C. However, two separate peaks in the (0001) pole figure are clearly visible in this case (Fig. 6b), with one group of grains perpendicular to ED and another one tilted at 57° to ED. It should be also noted that texture intensity was 6.2, which was much lower than in the previous I-ECAPed samples.

Optical microscope images, presented in Fig. 7, showed that grain size after final I-ECAP at 150 °C followed by heat treatment was dependent on the annealing temperature. First samples were kept in the furnace for 1 and 6 h; however no effect regarding mechanical properties and microstructure was observed for different times. Therefore, the results shown here refer only to the annealing time of 1 h. It is apparent from Fig. 7a that heat treatment at temperature equal to the last processing temperature (150 °C) did not introduce significant changes to the structure, as the measured grain size was ~0.9 μm. Since a linear intercept method was used here to measure the grain size, it could be a systematic difference. When annealing temperature was increased to 200 °C and above, grain growth was observed (Fig. 7b–d). The average grain size measured was 2.7, 3.5 and 4.7 μm after annealing at 200, 250, and 300 °C, respectively.

4.2. Mechanical properties

The extruded rod, which was supplied in as-fabricated state exhibited relatively high yield strength (220 MPa) and ultimate tensile strength (295 MPa) accompanied by limited ductility at room temperature as illustrated by tensile strain at fracture of 0.09 (Fig. 8a); true strain was used in this work as a measure of deformation level. Four passes of I-ECAP at 250 °C by routes A and B_C (part 1) reduced yield strength to 150 and 100 MPa, respectively, with simultaneous ductility enhancement to 0.14 and 0.22. Lowering temperature of I-ECAP to 200 °C in two subsequent passes increased yield strength and fracture strain to 205 MPa and 0.2, when route A was used (Fig. 8a). Moreover, a good hardening rate was obtained with ultimate tensile strength reaching 355 MPa just before fracture. Completely different results were obtained for route B_C. The flow stress curve after additional two passes at

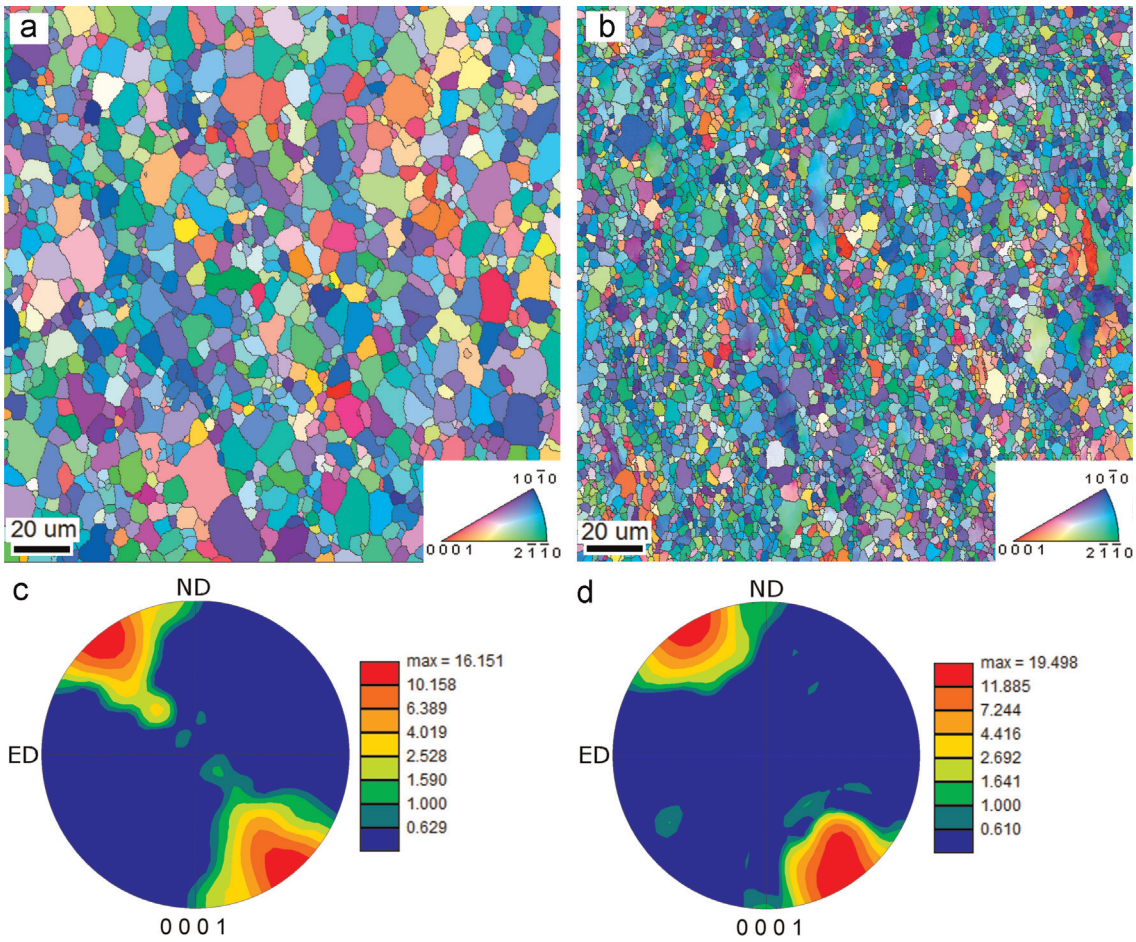

Fig. 4. EBSD maps and corresponding micro-textures of extruded samples after I-ECAP at 250 °C (a) and (c) and at 250 °C/200 °C (b) and (d) using route B_C.

200 °C looked almost exactly the same as after four passes at 250 °C (Fig. 8b). Microstructural and textural changes taking places during I-ECAP processing will be taken into account in Section 5 of this article to explain the observed discrepancy between mechanical responses of the billets subjected to different routes.

Mechanical properties after four passes at 250 °C using route C (part 2) were similar to route B_C, with the yield strength of 60 MPa and fracture strain of 0.22. The difference in flow behaviour of billets subjected to various routes of I-ECAP has been already discussed in our previous work [20]. In this study, an effect of heat treatment of I-ECAPed billet is investigated. It is apparent from Fig. 9 that significant improvement of ductility was obtained after annealing at 300 °C. True strain at break rose from 0.22 to 0.35, which is equivalent to 42% of engineering elongation, while yield stress was increased to 80 MPa. It is also worth noting that the sample was deformed uniformly almost to the fracture strain, reaching 340 MPa of the ultimate strength.

Yield strength of the supplied rolled plate (165 MPa) was lower than the extruded rod but fracture strain was 0.18, as shown in Fig. 10a. Four passes of I-ECAP at temperatures lowering from 200 °C to 150 °C (the third part of the experimental programme) significantly increased yield strength to 295 MPa without a major loss of ductility (true strain of 0.16). Although the hardening rate was lowered due to I-ECAP, the yield stress was continuously increasing during tensile testing and reached 360 MPa just before fracture. As shown in Fig.10b, post I-ECAP annealing for one hour influenced significantly strength and ductility at room temperature. The yield strength obtained after I-ECAP at 150 °C was slightly raised to 305 MPa along with fracture strain increased to 0.2 when annealing temperature was the same as during processing. Keeping the samples in the furnace heated to 200 °C and above resulted in decrease of yield strength to 265, 205, and 180 MPa after annealing at 200, 250, and 300 °C, respectively. However, reasonably good elongations were obtained with true strains at fracture exceeding 0.2 and even reaching 0.3 after heat treatment at 250 °C. Extraordinary mechanical properties were achieved after annealing at 150 and 200 °C as both strength and ductility were simultaneously improved compared to the commercially available rod and plate, used in this work as reference materials.

5. Discussion

5.1. Effects of grain size and texture on mechanical properties

Grain refinement in billets subjected to I-ECAP at 250 °C is related to temperature rather than processing route. The difference between mean grain sizes obtained by routes A and B_C was within 1 μm, which does not explain significantly different mechanical responses of both samples. Therefore, higher yield strength of the billet processed by route A is attributed to the strong texture with *c*-axes of hcp cells almost perpendicular to tensile direction while low yield strength after route B_C is a result of hcp cells alignment favourable for slip on basal plane; this behaviour was already analysed for routes A, B_C and C in our previous article [20].

Further processing at 200 °C resulted in a very similar grain refinement to 2.5 μm for both routes and the previous difference in grain size was levelled. Texture after processing by route B_C at 200 °C was not changed significantly as basal planes were still in positions favourable for basal slip which was confirmed by almost

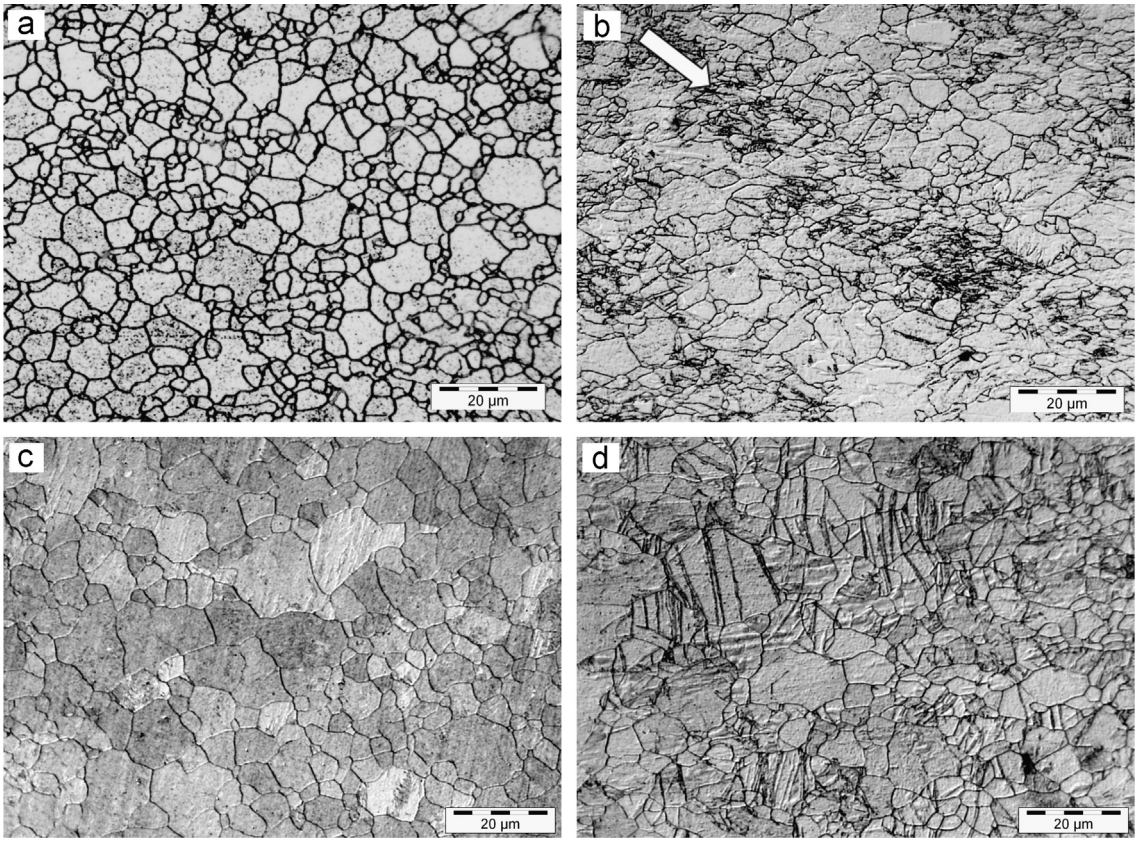

Fig. 5. Optical microscope images of extruded samples after four passes of I-ECAP at 250 °C by route C (a) and subsequent annealing for 6 h at 300 °C (c), corresponding microstructures after tensile testing to true train 0.15 are shown in (b) and (d), respectively.

the same flow stress curve as after four passes at 250 °C. It clearly shows that strong basal texture produced by route B_C does not allow taking advantage of grain reduction in terms of strengthening of the alloy. It has also revealed that Hall–Patch [23,24] relation, expressing yield strength increase along with grain refinement, cannot be fulfilled in magnesium alloys when the Schmid factor for slip on basal plane is significantly larger than for any other mode of deformation. Theoretical analysis carried out by Kleiner and Uggowitzer [25] showed that Schmid factor for slip on basal plane reaches its maximum when *c*-axes of hexagonal cells are tilted at 57°, which corresponds very well to results obtained in this work by route B_C.

In contrast to route B_C, route A exhibited significant yield strength increase from 150 MPa after I-ECAP at 250 °C to 205 MPa after further processing at 200 °C. Although grain size reduction from 4 μm to 2.5 μm can be a reason for strength increase, it does not explain ductility enhancement to 0.2 of fracture strain. It is claimed here that distinctive texture produced after I-ECAP at 200 °C by route A (Fig. 3d) resulted in better ductility. Two overlapping peaks can be distinguished in the corresponding (0001) pole figure, with *c*-axes tilted at 75° and 62° to ED. Combination of 75° orientation of grains and their small size (2.5 μm) gave rise to yield strength improvement to 205 MPa while another set of grains, with basal planes tilted at 62° to ED, was deformed mainly by basal slip which enabled ductility enhancement.

The conclusion drawn from this part of experimental work is that I-ECAP by route A is more effective in improving strength (without losing ductility) than commonly used route B_C. This can be explained by textural effects as it is shown that texture plays a dominant role over grain size in controlling mechanical properties. On the other hand, strongly textured AZ31B alloy, with *c*-axes of hexagonal cells inclined at ~57° to tensile direction, can be a possible strategy for ductility improvement when strength is not of a great importance.

5.2. Ductility enhancement by heat treatment

A large elongation, exceeding 40%, after ECAP via route B_C followed by annealing was reported by Mukai et al. [10]. The obtained ductility enhancement, accompanied by reduction of yield strength, also observed in this work (increase of true strain at fracture from 0.22 to 0.35), was attributed to grain growth to 15 μm during 24 h heat treatment at 300 °C. This observation was confirmed by Agnew et al. [26] who showed that post-deformation annealing did not change strong basal texture obtained after ECAP, only grain size was increased to 19 μm. The authors of both papers noticed that 45° tilting of *c*-axes with reference to ED enabled slip on basal plane during tension which gave rise to ductility enhancement. However, the papers did not explain how grain growth during annealing improved formability compared to as-ECAPed state.

Our previous research showed that route B_C can lead to distortion of billet cross section [27], which has not been observed for route C while mechanical properties after both processing paths were very similar [20]. Therefore, in order to study the problem of increased ductility, I-ECAP experiments were conducted at 250 °C using route C followed by annealing. Grain size after I-ECAP was reduced to ~4.5 μm and the following heat treatment for 6 h at 300 °C increased it to only 6 μm. Based on these results, the effect of grain growth during annealing can be considered negligible from the view point of mechanical properties. One can also recall that texture is not affected by annealing, according to [26]. Although microstructure looked very similar before and after heat treatment, ductility was significantly improved from 0.22 to 0.35

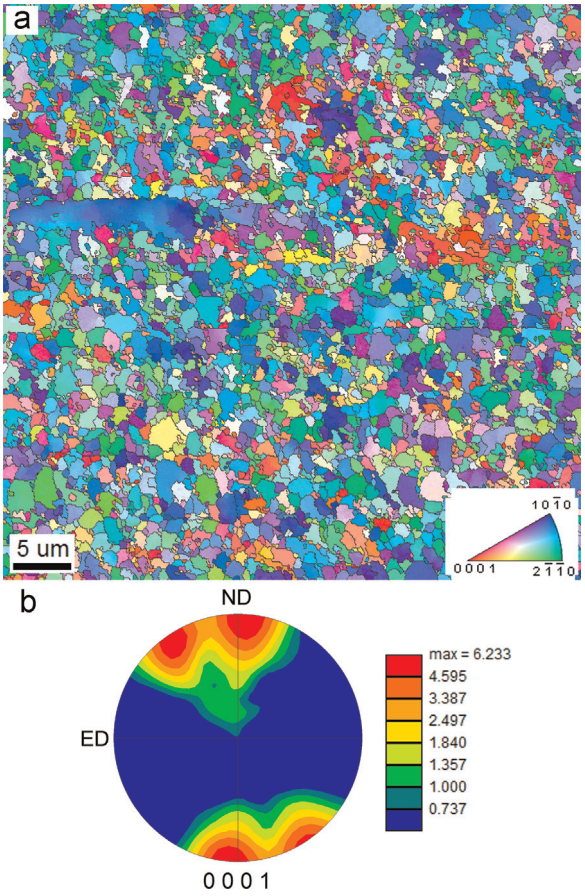

Fig. 6. EBSD map and micro-texture of rolled sample after four I-ECAP passes by route A with a final temperature of 150 °C.

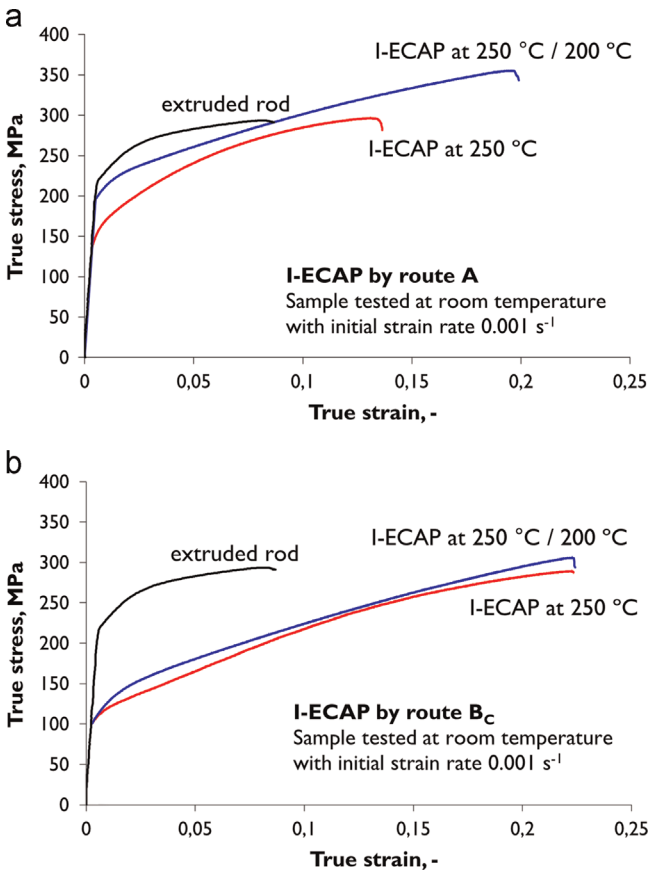

Fig. 8. Tensile flow stress curves of extruded samples subjected to I-ECAP by routes A (a) and B_C (b) at 250 °C and 250 °C/200 °C.

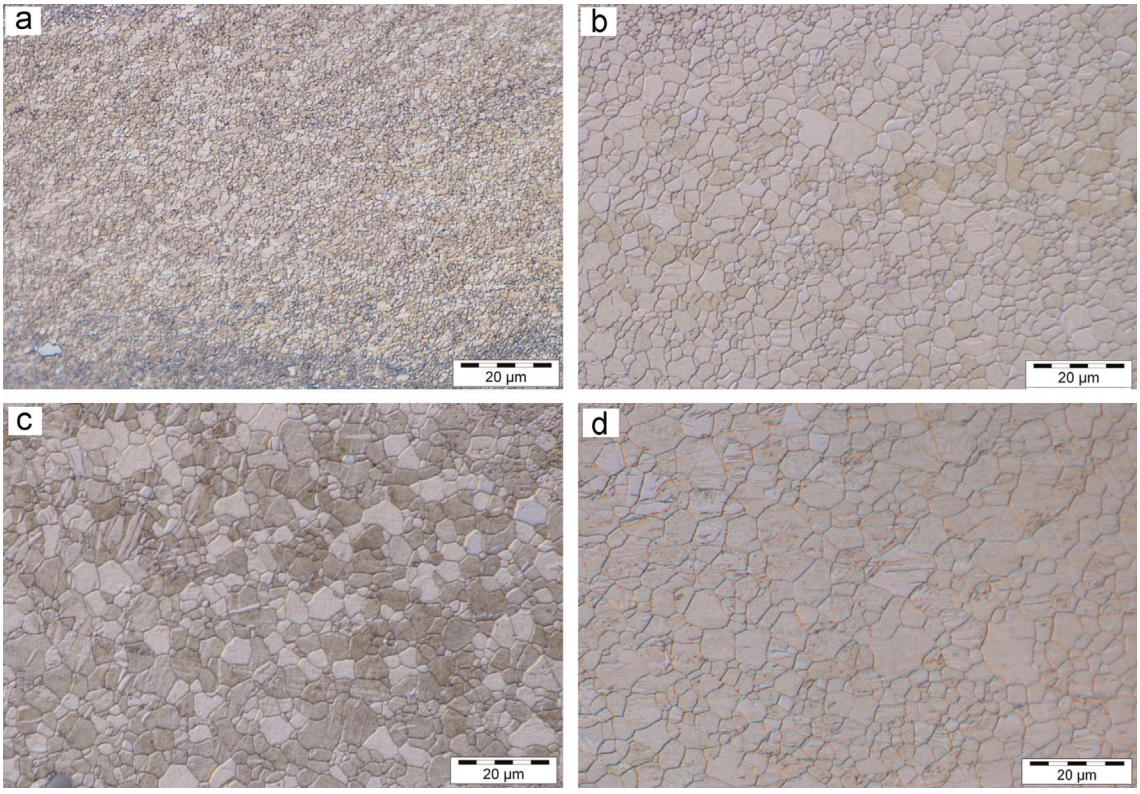

Fig. 7. Optical microscopy images of rolled samples after final pass of I-ECAP at 150 °C followed by annealing for 1 h at 150 °C (a), 200 °C (b), 250 °C (c), and 300 °C (d).

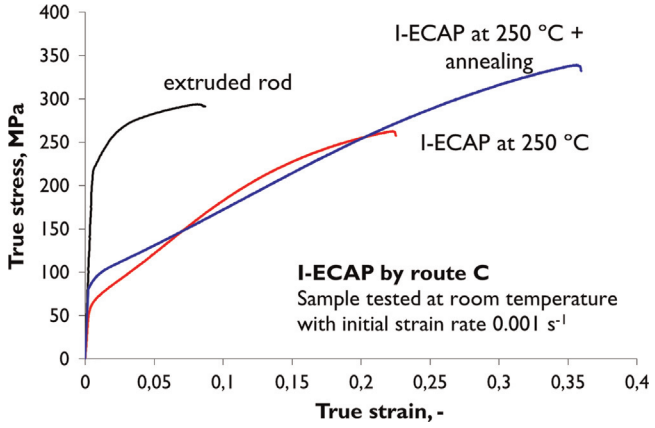

Fig. 9. Tensile flow stress curves of extruded samples after four passes of I-ECAP at 250 °C by route C and after subsequent annealing for 6 h at 300 °C.

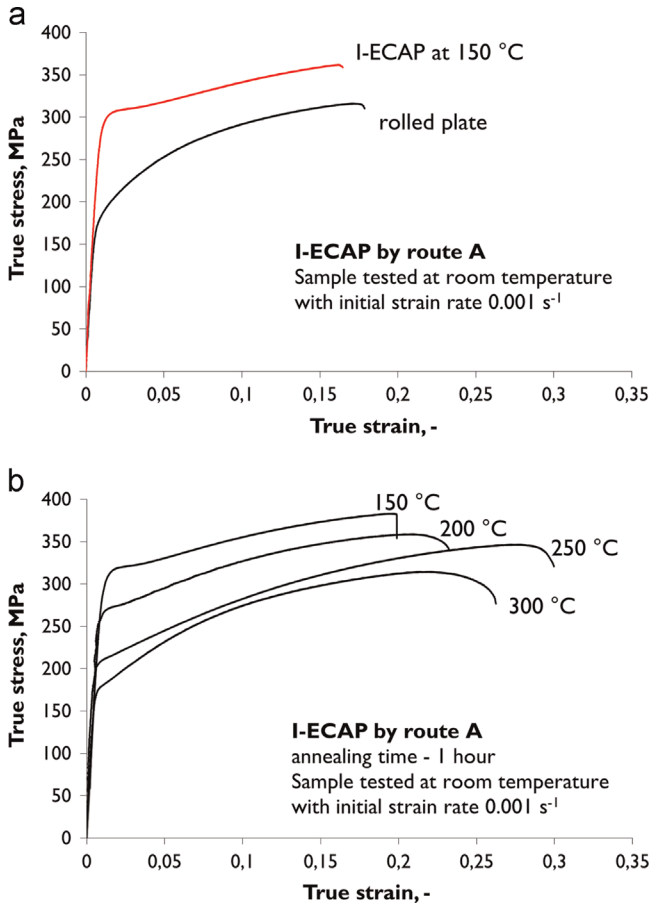

Fig. 10. Tensile flow stress curves of rolled samples after four passes of I-ECAP with final two conducted at 150 °C (a) and after subsequent annealing for 1 h at 150, 200, 250 and 300 °C (b).

of true strain, which is very similar to the values found in the literature [10,26]. However, grain growth related explanation for ductility enhancement proposed in those articles cannot be applied here as the grain size was much smaller in our experiment.

An alternative explanation can be offered by analysing more subtle features of the structure. A necklace-like structure (Fig. 5a) is commonly observed when dynamic recrystallization (DRX) takes place and this process is believed to control grain refinement of magnesium alloys in ECAP [11,16,28,29]. However, the heterogeneous microstructure can result in localization of strain along colonies of fine grains (Fig. 5b), as it was reported in the past [30]. Post-I-ECAP annealing resulted in homogenization of grain size distribution since necklace-like structure was no longer present after six hours in the furnace (Fig. 5c). As a consequence, shear banding, which led to fracture at true strain of 0.22, was avoided and further deformation to true strain of 0.35 was enabled.

The dominant role of basal slip during tensile testing of the annealed samples emphasized in the literature [26] should be discussed here as well. Despite I-ECAPed texture indicating importance of this kind of deformation, it was shown that microstructure of the annealed sample was severely twinned at true strain 0.15. It is especially interesting as twinning is usually expected to decrease ductility [31–33] while in this work it was revealed in the sample, which exhibited extraordinary elongation along tensile direction. EBSD analysis of the deformed structure (Fig. 11) showed that almost all of the twins are {10–12} twins with 86° grain boundaries, which facilitate extension along *c*-axis (so called *tensile twins*). This twinning variant has been already reported in the literature as a deformation mechanism giving rise to improvement of uniform elongation in tensile samples tested along radial direction of the extruded rod of AZ31 [34]. Thus, it seems that slip on the basal plane is the main deformation mechanism at the initial stage of tension. However, further strain cannot be accommodated by the basal slip only and tensile twining is activated, which leads to ductility enhancement. Additionally, good hardening rate of the annealed sample can be attributed to the twinning occurrence since rotation of basal planes by 86° increases stress and twin boundaries can also act as barriers for dislocation movement. Finally, anisotropic mechanical properties of the strongly textured I-ECAPed and annealed sample should be noted here since Agnew et al. [26] showed that extraordinary elongation along ED is not as spectacular during testing in other directions, which should be taken into account during forming of the I-ECAPed billets.

5.3. Strength improvement

The results obtained in the first part of experimental campaign showed that route A at 250 °C/200 °C could be effective in strength improvement of AZ31B magnesium alloy despite the yield strength (205 MPa) being still lower than after direct extrusion (220 MPa). Since our previous research revealed that smaller initial grain size of a magnesium alloy allows processing at a lower temperature [22], a procedure of gradual temperature decrease was applied to the fine-grained billets obtained by hot rolling in order to conduct I-ECAP below 200 °C. I-ECAP at 150 °C was successful in refining grain size to 0.8 μm as it was measured from EBSD map. Generation of submicron structure resulted in significant yield strength increase to 295 MPa, which was much higher than in the cases of extruded rod and rolled plate.

The role of texture cannot be neglected as well since it was shown in this work that texture produced by route A was more effective in strength improvement than route B_C. The pole figure obtained after processing at 150 °C was similar to that for 200 °C but with more visible peaks of maximum intensities. Although initial textures of the extruded and rolled samples were different, large strain introduced during I-ECAP via route A resulted in the very similar final texture. Interestingly, a very similar alignment of shear patterns on the ED–ND plane after four passes of ECAP was predicted by a model developed by Langdon [35]. He calculated that a maximum angle between shear patterns introduced by subsequent ECAP passes reaches 37° after fourth pass, which is in a very good agreement with the obtained pole figure (Fig. 6b), where an angle between the two peaks of maximum intensities is 35–40°. It supports the idea that the produced texture is related directly to the processing route.

The same conclusion as for the billet subjected to I-ECAP at 250 °C/200 °C by route A can be drawn for 150 °C, namely grains oriented almost perpendicularly to ED attributed to strength increase while 57° orientation helped with keeping reasonable ductility at

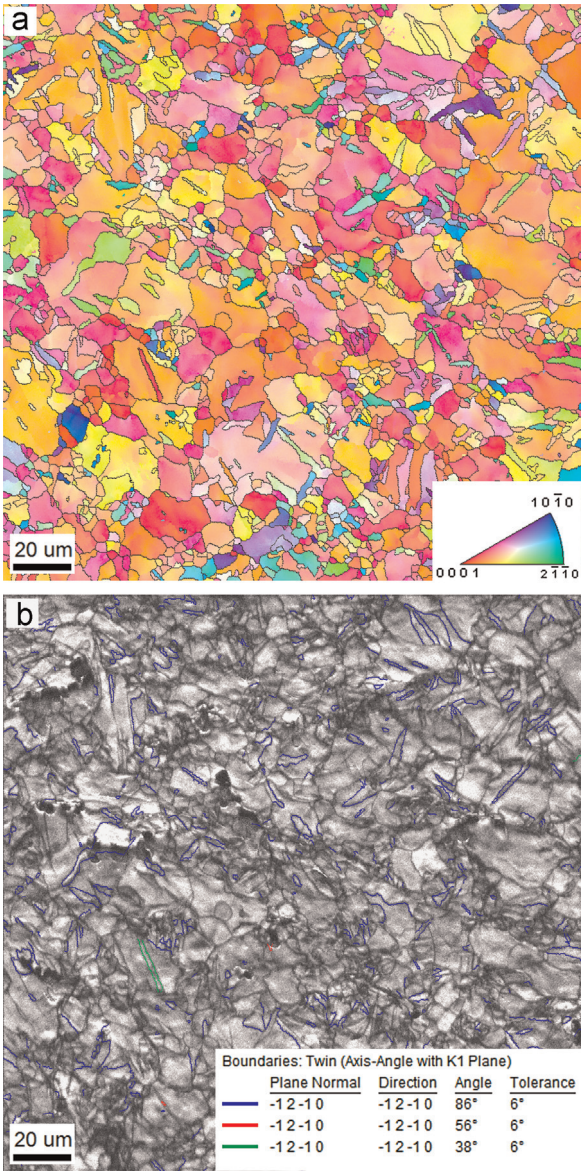

Fig. 11. EBSD (a) and twin grain boundaries (b) maps of the extruded and I-ECAPed sample (4 passes at 250 °C by route C) followed by annealing (6 h at 300 °C) pulled to true strain of 0.15. Tensile direction was horizontal.

room temperature due to activation of basal slip. It can be concluded that combination of ultra-fine grain structure and proper texture is required to increase strength to ~300 MPa without losing ductility. Moreover, much lower maximum intensity (~6.2) of the (0001) pole figure after processing at 150 °C than for any other I-ECAPed sample studied in this work is promising with respect to isotropy of mechanical properties.

Heat treatment at 200 °C and above of billets previously I-ECAPed at 150 °C resulted in grain growth and corresponding decrease of strength at room temperature. The main mechanism for grain growth during post-deformation annealing was static recrystallization. However, Barnett and Beer [36] claimed that microstructure restoration can be also attributed to continued growth of nuclei formed by dynamic recrystallization during plastic deformation. Despite the annealing temperature in their study being higher (400 °C), it could have been also the case of the samples tested in this work.

Texture produced by I-ECAP was assumed to remain unaffected by the following heat treatment, according to the experiments conducted by Agnew et al. [26]. Thus, the grain size increase with annealing temperature was shown to have a crucial effect on yield strength at room temperature. One hour in the furnace at 300 °C was enough to reverse structural changes introduced by I-ECAP and return to almost the same mechanical properties as in the as-supplied state (after rolling). Interesting results were obtained after annealing at 250 °C where a significant ductility enhancement was obtained (0.3 of true strain) with a reasonably high yield stress of 205 MPa. However, we could not find an explanation for the lower ductility after heat treatment at 300 °C compared to that at 250 °C; further research will be required to investigate this behaviour. Finally, it was shown that only annealing at 150 °C allowed keeping moderate strength (even slightly increased) of 305 MPa with a relatively good true strain at fracture of 0.2. We postulate that ductility enhancement from 0.16 after I-ECAP to 0.2 after subsequent annealing should be attributed to reduction of internal stresses due to annihilation of dislocations. Additionally, low annealing temperature allowed keeping submicron structure which resulted in sustaining of yield strength with a decent hardening response. The results presented here are in good agreement with the work by Stráská et al. [37] who showed that structure of ultrafine-grained AZ31 (~0.9 μm) was stable after annealing at 170 °C and grain growth was observed from 190 °C.

6. Conclusions

Wrought magnesium alloy AZ31B was characterized after different versions of thermo-mechanical treatment, including incremental equal channel angular pressing (I-ECAP) and annealing. Conclusions from the conducted study are listed below.

1. Texture plays a dominant role in controlling mechanical properties after I-ECAP. It was shown that grain size reduction to ~2.5 μm has not changed mechanical properties of the billet processed by route B_C while strength improvement from 150 to 205 MPa was obtained after route A, despite the same final grain size as after route B_C.
2. The room temperature ductility of AZ31B can be increased from 0.22 of true strain at fracture after I-ECAP at 250 °C via route C to 0.35 (equivalent to 42% elongation) after subsequent annealing at 300 °C. The achieved ductility enhancement was attributed to: (1) the facilitation of basal slip due to texture developed during I-ECAP and (2) the homogenization of grain size distribution after heat treatment leading to suppression of shear banding. Tensile twinning was shown to play an important role in accommodating large strain during tensile testing of the annealed sample.
3. The yield strength of AZ31B alloy was increased to 305 MPa by I-ECAP at 150 °C using route A followed by annealing at the same temperature. Additionally, decent hardening response was obtained with ultimate tensile stress of 380 MPa and good ductility, expressed as 0.2 of true fracture strain.
4. I-ECAP was confirmed to be a promising tool for processing of continuous magnesium alloy billets leading to a significant improvement of their mechanical properties.

Acknowledgments

Financial support from Carpenter Technology Corporation is kindly acknowledged. Part of this research was supported by the Engineering and Physical Sciences Research Council, United Kingdom [Grant no. EP/G03477X/1].

References

[1] S. Schumann, H.E. Friedrich, in: H.E. Friedrich, B.L. Mordike (Eds.), Magnesium Technology: Metallurgy, Design Data, Applications, Springer-Verlag, Heidelberg, 2006, pp. 499–568.
[2] F.H. Froes, D. Eliezer, E. Aghion, in: H.E. Friedrich, B.L. Mordike (Eds.), Magnesium Technology: Metallurgy, Design Data, Applications, Springer-Verlag, Heidelberg, 2006, pp. 603–619.
[3] M.P. Staiger, A.M. Pietak, J. Huadmai, G. Dias, Biomaterials 27 (2006) 1728–1734.
[4] V.M. Segal, V.I. Reznikov, A.E. Drobyshevskiy, V.I. Kopylov, Russ. Metall. (Met.) 1 (1981) 99–105.
[5] V.M. Segal, Mater. Sci. Eng. A 197 (1995) 157–164.
[6] A. Rosochowski, L. Olejnik, in: E. Cueto, F. Chinesta (Eds.), Proceedings of the 10th International Conference on Material Forming, Esaform 2007, 18–20 April 2007, Zaragoza, Spain, American Institute of Physics, 2007, vol. 907, pp. 653–658.
[7] A. Rosochowski, L. Olejnik, Mater. Sci. Forum 674 (2011) 19–28.
[8] A. Rosochowski, L. Olejnik, M. Richert, Mater. Sci. Forum 584–586 (2008) 108–113.
[9] A. Rosochowski, M. Rosochowska, L. Olejnik, B. Verlinden, Steel Res. Int. 81 (2010) 470–473.
[10] T. Mukai, M. Yamanoi, H. Watanabe, K. Higashi, Scr. Mater. 45 (2001) 89–94.
[11] S.X. Ding, C.P. Chang, P.W. Kao, Metall. Mater. Trans. A 40 (2009) 415–425.
[12] J. Jiang, A. Ma, N. Saito, Z. Shen, D. Song, F. Lu, Y. Nishida, D. Yang, P. Lin, J. Rare Earths 27 (2009) 848–852.
[13] D. Orlov, K.D. Ralston, N. Birbilis, Y. Estrin, Acta Mater. 59 (2011) 6176–6186.
[14] W.J. Kim, C.W. An, Y.S. Kim, S.I. Hong, Scr. Mater. 47 (2002) 39–44.
[15] S. Seipp, M.F.-X. Wagner, K. Hockauf, I. Schneider, L.W. Meyer, M. Hockauf, Int. J. Plast. 35 (2012) 155–166.
[16] M. Janecek, M. Popov, M.G. Krieger, R.J. Hellmig, Y. Estrin, Mater. Sci. Eng. A 462 (2007) 116–120.
[17] S.R. Agnew, P. Mehrotra, T.M. Lillo, G.M. Stoica, P.K. Liaw, Mater. Sci. Eng. A 408 (2005) 72–78.
[18] K. Bryla, J. Dutkiewicz, P. Malczewski, Arch. Mater. Sci. Eng. 40 (2009) 17–22.
[19] L. Jin, D. Lin, D. Mao, X. Zeng, B. Chen, W. Ding, Mater. Sci. Eng. A 423 (2006) 247–252.
[20] M. Gzyl, A. Rosochowski, R. Pesci, L. Olejnik, E. Yakushina, P. Wood, Metall. Mater. Trans. A 45 (2014) 1609–1620.
[21] A. Rosochowski, L. Olejnik, M. Richert, Mater. Sci. Forum 584–586 (2008) 139–144.
[22] M. Gzyl, A. Rosochowski, L. Olejnik, A. Reshetov, Key Eng. Mater. 611–612 (2014) 573–580.
[23] E.O. Hall, Proc. Phys. Soc. Lond. Sect. B 64 (1951) 747–753.
[24] N.J. Petch, J. Iron Steel Inst. 174 (1953) 25–28.
[25] S. Kleiner, P.J. Uggowitzer, Mater. Sci. Eng. A 379 (2004) 258–263.
[26] S.R. Agnew, J.A. Horton, T.M. Lillo, D.W. Brown, Scr. Mater. 50 (2004) 377–381.
[27] M. Gzyl, A. Rosochowski, E. Yakushina, P. Wood, L. Olejnik, Key Eng. Mater. 554–557 (2013) 876–884.
[28] R.B. Figueiredo, T.G. Langdon, J. Mater. Sci. 44 (2009) 4758–4762.
[29] M. Gzyl, A. Rosochowski, A. Milenin, L. Olejnik, Comput. Methods Mater. Sci. 13 (2013) 357–363.
[30] S.E. Ion, F.J. Humphreys, S.H. White, Acta Metall. 30 (1982) 1909–1919.
[31] B.C. Wonsiewicz, W.A. Backofen, Trans. Metall. Soc. AIME 239 (1967) 1422–1431.
[32] T. Al-Samman, G. Gottstein, Mater. Sci. Eng. A 488 (2008) 406–414.
[33] M. Gzyl, R. Pesci, A. Rosochowski, S. Boczkal, L. Olejnik, J. Mater. Sci. 50 (2015) 2532–2543.
[34] M.R. Barnett, Mater. Sci. Eng. A 464 (2007) 1–7.
[35] T.G. Langdon, Mater. Sci. Eng. A 462 (2007) 3–11.
[36] A.G. Beer, M.R. Barnett, Scr. Mater. 61 (2009) 1097–1100.
[37] J. Stráská, M. Janeček, J. Čížek, J. Stráský, B. Hadzima, Mater. Charact. 94 (2014) 69–79.